INL/RPT-24-76179
Revision 0

Light Water Reactor Sustainability Program

Evaluating Energy Storage Options and Costs for Consistent Energy Supply to Non-Electric Sectors

January 2024
U.S. Department of Energy
Office of Nuclear Energy

INL/RPT-24-76179
Revision 0

Evaluating Energy Storage Options and Costs for Consistent Energy Supply to Non-Electric Sectors

So-Bin Cho
Rami M. Saeed
Idaho National Laboratory

January 2024

Idaho National Laboratory
Light Water Reactor Sustainability
Idaho Falls, Idaho 83415

http://lwrs.inl.gov

Prepared for the
U.S. Department of Energy
Office of Nuclear Energy
Under DOE Idaho Operations Office
Contract DE-AC07-05ID14517

ABSTRACT

This study investigates the different options for coupling thermal energy (TES) systems to a pressurized light water reactor (PWR) and assesses the competitiveness of PWR-TES systems considering different technological constraints, industrial requirements, and market conditions. The present work draws on heat balance analysis results obtained from extracting 30% of the reactor heat from a 4-loop Westinghouse PWR plant. Previous research has determined that two-tank molten salt TES designs are one of and perhaps the most practical option for delivering PWR heat to industrial customers.

To assess the competitiveness of PWR-TES systems, our study examined 40 different cases derived from an array of potential pathways for PWR-TES systems, including different modes of heat extraction and varying types of industrial customers. The results show that the economics of PWR-TES systems are largely determined by mean electricity price of the market where the PWR-TES systems are introduced. This effect is more pronounced when the plant operates in a fixed 30% heat extraction mode. Additionally, when the optimal TES capacity is sized to accommodate a 1-hour charge duration, equivalent to 1095 MWht, the TES system typically operates as a buffer. The heat diverted to the TES is quickly delivered to industrial customers, rather than being stored for future energy arbitrage purposes. Results showing an optimal TES capacity greater than 1095 MWht were typically obtained at price points where revenue from heat was approximately equivalent to that of electricity.

To further enhance our analysis, we differentiated heat price levels across two distinct electricity markets, the Electricity Reliability Council of Texas (ERCOT) and the Pennsylvania-New Jersey-Maryland (PJM) Interconnection, to evaluate sensitivities and identify favorable market conditions for PWR-TES systems. Over a heat price range of 7-18 $/MWht, a variable 0-30% heat extraction mode generally led to a positive change in net present values (NPVs) in both markets, demonstrating robust marketability for TES operations. Imposing a minimum heat dispatch constraint resulted in poorer economics because it impaired the ability of the TES system to achieve maximum revenue according to dynamic electricity prices. Our sensitivity analysis also indicated a high heat price level (> $13/MWht) may reduce the need for TES because there are frequent instances where selling heat directly to industrial consumers could yield more profit compared to the generation of electricity.

The insights obtained from this study could provide valuable guidance for integrating PWR-TES systems with industrial consumers, particularly those with diverse heat requirements. Future research should focus on enhancing the heat balance analysis for variable heat extraction rates. Consideration should also be given to upgrading current turbines to maximize the economic impact of PWR-TES systems in markets with low-electricity prices.

EXECUTIVE SUMMARY

Background

Non-electric applications of nuclear heat have attracted interest as a cleaner alternative to conventional process heat traditionally sourced by fossil fuels. Previous work led by the Department of Energy's (DOE's) Light Water Reactor Sustainability (LWRS) Program identified key impacts of 30% thermal power extraction on a generic Westing house 4-loop pressurized light water reactor (PWR) design. Coupling thermal power extraction with thermal energy storage offers greater benefits in terms of flexibility and arbitrage between electricity and thermal energy markets. Accordingly, Idaho National Laboratory (INL) has evaluated the cost of sensible thermal energy storage (TES) at various temperatures from existing and advanced nuclear reactor designs for different non-electric applications. With its proven technical maturity, sensible TES can be readily tailored for specific use-cases by selecting an appropriate heat transfer fluid (HTF) and optimizing the storage capacity. In addition to the benefits mentioned above, sensible TES also provides a secondary source of thermal inertia in case of PWR failure, and it can improve the peak electricity generation capacity.

While TES systems cover a wide array of heat inputs by utilizing different storage materials and energy conversion techniques, this study focuses solely on two-tank TES configurations where the hot and cold HTF is stored separately. This approach has the advantage of scalability and applicability, ensuring constant power and temperature throughout the entire charge and discharge process. This analysis focuses on molten salt HTFs due to their attractive characteristics, including relatively low cost, high volumetric heat capacity, and medium- and high-temperature operating ranges (200 - 600 °C) in low-pressure conditions.

Selection of Molten Salts for PWR-TES Coupling

The performance of molten salts as HTFs for PWR plants is largely dependent on the temperature of the available heat, which is in the range of 270-280 °C and establishes the upper temperature limit of the fluid in the hot storage tank. The lower temperature limit of the fluid in the cold storage tank must be 40-100 °C above the melting point of the salt to prevent issues related to salt freezing. Other important salt selection parameters include thermal stability, heat capacity, viscosity, thermal conductivity, corrosivity, and cost. These considerations narrow the best molten salt options for PWR-TES coupling to Hitec, Hitec XL, Solar Salt, $LiNaKNO_3$, $LiNaKCaNO_3$, and $LiNO_3$ (lithium nitrate). Among these salts, corrosivity is a particular concern. Simulations and experimental studies have suggested various corrosion mitigation strategies such that all these salts are considered suitable for TES plants operating below 400 °C.

PWR-Two Tank Molten Salt TES System Designs

Building on prior research at INL, two TES coupling designs were explored. The first design, shown in Figure S-1, employs an intermediate heat exchanger to use main steam to heat molten salt entering the hot storage tank. An option with this design is to bypass the TES system by directly sending steam to the heat customer when the TES system is fully charged. The second TES coupling design adds a turbine-generator system to the TES system, so that the TES system can produce electricity beyond that produced by the PWR. The second design increases the maximum electricity generation capacity of the plant for peak grid power demand but has lower efficiency due to exergy losses in the TES system. In each of the designs, the temperature of the salt in the cold tank is maintained at 180 °C.

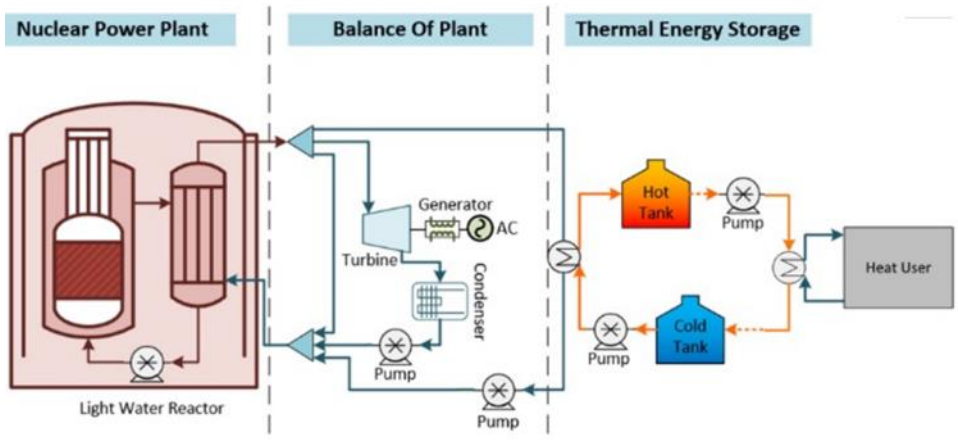

Figure S-1. One option to couple a TES with a PWR utilizing an intermediate heat exchanger.

Bilateral Heat Energy Market for Homogenous Industrial Users

Contrary to electricity markets that are characterized by multiple buyers and sellers, heat energy transactions typically occur via bilateral contracts at a fixed price between the supplier and customer. Coupled PWR-TES systems interact with both markets, which allows them to seek energy arbitrage opportunities through bilateral heat contracts. Table S-1 lists possible market options for PWR-TES systems in dual heat and electricity markets. This study prioritizes heat markets characterized by minimum heat demand and unrestricted selling capacity. In these heat market settings, homogeneous heat consumers were assumed to own their boilers and have the ability to control their outputs, implying that PWR-TES system can dispatch any amount of heat at the fixed heat price.

Table S-1. The heat extraction modes and their implications of introducing TES in scenarios of heat procurement at a fixed price within an electricity market with variable pricing.

Heat dispatch contract	Constant heat demand	Scheduled heat demand	Minimum heat demand	Unrestricted heat selling capacity
Fixed 30% dispatch	No energy arbitrage opportunities for TES	Market potential for TES	Market potential for TES	Market potential for TES
Variable 0-30% dispatch	Market potential for TES	Market potential for TES	Market potential for TES	Market potential for TES

Summary of HERON Case Setup and Results

The Risk Analysis Virtual ENvironment (RAVEN) and Holistic Energy Resource Optimization Network (HERON) frameworks were used to derive the cost-optimal interaction between technological constraints and optimal superset capacities, and various performance attributes. The optimization process adjusts the TES capacity, projected mean NPV, electricity and heat transactions but does not adjust the PWR primary loop and its existing BOP because those items are pre-existing equipment. Conversely, components integral to the coupling—namely, the charging, discharging (including secondary BOP considerations), and TES supersets —possess fixed or a range of capacity values, thereby resulting in varying capital expenditure based on the corresponding superset cost functions. The analysis specifically addresses the incremental variations in net present value (NPV) due to possible additional investments in installing charge, discharge, and TES supersets. The analysis includes 40 cases that are based on five possible scenarios: (1) a PWR plant operating as Business as Usual (BAU) with no TES; (2) a PWR-TES with a separate turbine-generator system for electricity-only markets (no thermal power dispatch); directly supplying industrial heat to customers with stored heat energy from (3) fixed and (4) variable thermal

power dispatch operations, and (5) heat dispatch is constrained to always remain above a minimum threshold of either 500 or 800 MWt to meet customer needs. In Table S-2, these scenarios are denoted as BAU, TES+BOP, Fixed 30% heat dispatch, Variable 0-30% heat dispatch, and Min. heat dispatch constraint, respectively.

Table S-2. Modeled scenarios for different markets, technological assumptions, and simulation settings.

Scenario	Market	Heat price [$/MWht]	Minimum heat supply to industrial customers [MWt]	Storage charge duration [hour]
BAU	ERCOT	-	-	-
	PJM	-	-	-
TES+BOP [1]	ERCOT	-	-	-
	PJM	-	-	-
Fixed 30% heat dispatch	ERCOT	7, 10, 13, 16	0	1-12 hours with 1-hour intervals
	PJM	7, 10, 13, 16	0	1-12 hours with 1-hour intervals
Variable 0-30% heat dispatch	ERCOT	7, 10, 13, 16, 19, 22, 25, 28	0	1-12 hours with 1-hour intervals
	PJM	7, 10, 13, 16	0	1-12 hours with 1-hour intervals
Min. heat dispatch constraint[1]	ERCOT	7, 10, 13, 16	500, 800	1-12 hours with 1-hour intervals
	PJM	7, 10, 13, 16	500, 800	1-12 hours with 1-hour intervals

[1] *The heat extraction models for TES+BOP and Min. heat dispatch constraint scenarios were allowed to vary within their constraints.* **NOTE:** TES was modeled with a round-trip efficiency (RTE) of 90%, and incorporates a periodic condition, thus ensuring a fixed storage level (i.e., 75% TES capacity) at both the start and end of each simulation timestep.

Figure S-2 and Figure S-3 summarize trends and key parameters for each scenario in the ERCOT and PJM markets. For simplicity, only the cases with the highest NPV from Table S-2 are shown. Each row (representing individual market partition) is contrasted with the corresponding BAU scenario and TES+BOP scenario to highlight the potential economic advantages derived from adopting a TES for industrial heat supply. Figure S-2 presents the extra capital investments dedicated to this transition, clarifying the absence of corresponding optimal capacities (located on the top of Figure S-2A and C) and costs in the minus NPV column for the BAU scenario and the TES+BOP scenario (Figure S-2B and D).

The results show that the economics of PWR-TES systems are largely determined by the mean electricity price of the market where the PWR-TES systems are introduced. The design with TES and secondary BOP for peak electricity dispatch showed more economic potential in the ERCOT market compared to its BAU scenario, resulting in a positive change in NPV. The same configuration in the PJM market resulted in a negative change in NPV due to the relatively low electricity prices in the PJM market. In both markets, the capital recovery of the TES+BOP system is limited by the low thermal-to-electric conversion efficiency of the secondary BOP (27.53%). For designs in which the optimal TES capacity is equivalent to a 1-hour charge duration or 1095 MWht, the TES system operates primarily as a buffer. The heat dispatched to the TES is quickly delivered to industrial customers, rather than being stored for future energy arbitrage purposes. Optimized scenarios for which the TES capacities were greater than 1095 MWht were typically obtained at price points where the costs of heat and electricity were approximately equivalent. Interestingly, within the PJM market, PWR-TES systems outperformed the TES+BOP scenario, resulting in a higher mean NPV at a heat price of $10/MWht (Table 9).

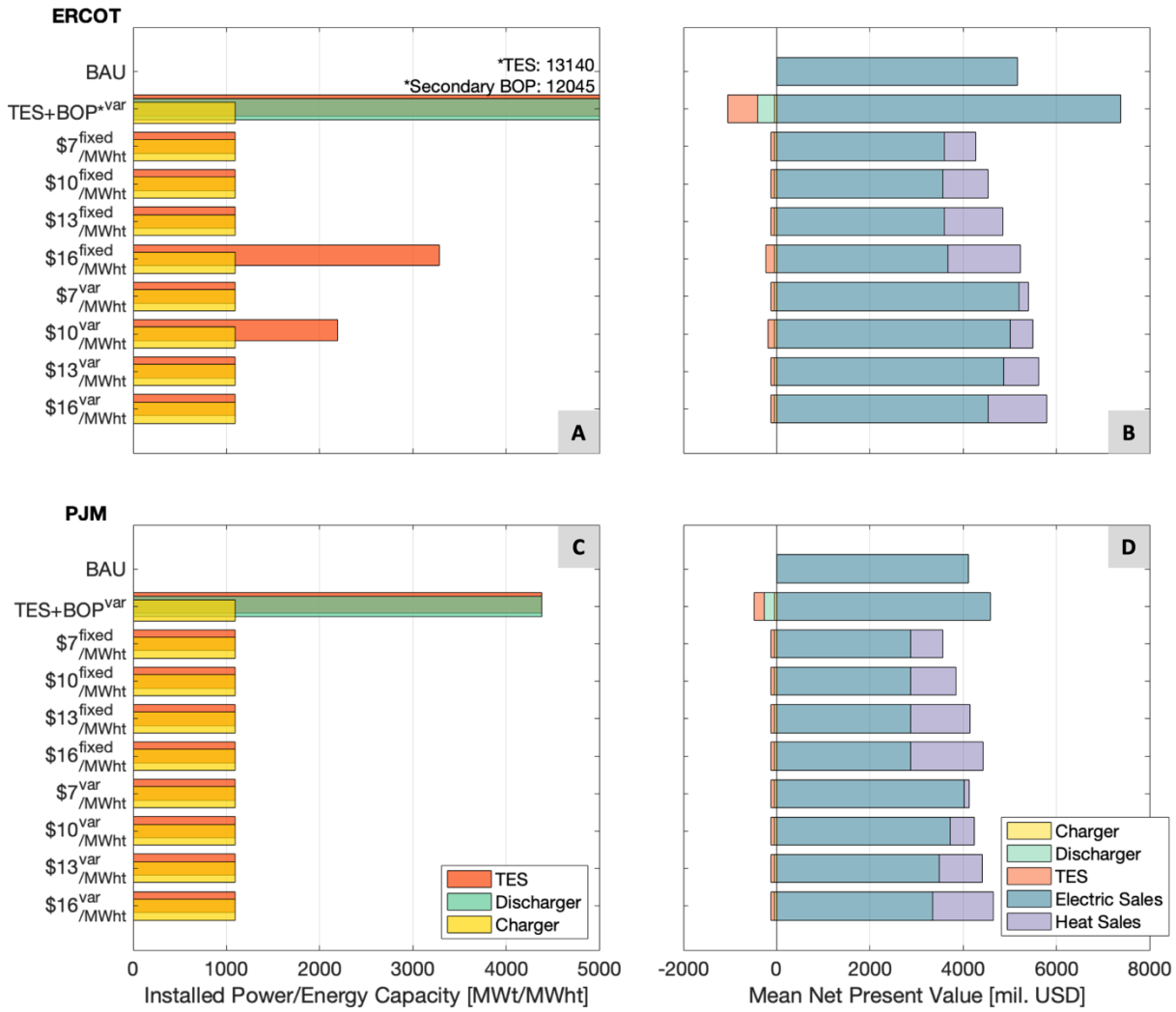

Figure S-2. HERON-optimized cases for the PWR-TES coupling superset capacity (left), NPV (right), and energy transaction (right). Note that the scenarios for "Fixed 30% heat dispatch" and "Variable 0-30% heat dispatch" are denoted as 'fixed' and 'var' in superscript, respectively; The heat dispatch mode for TES+BOP is set at a variable range of 0-30% (denoted as ‘var’ in superscript).

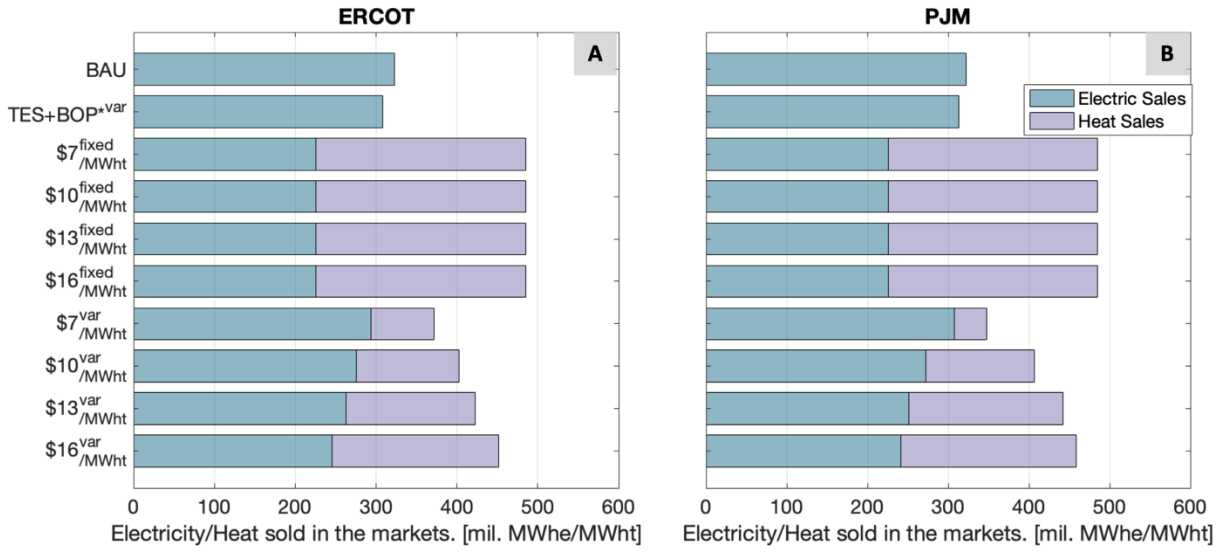

Figure S-3. Comparison of electricity and heat transactions under different scenarios and markets.

Across all markets, a fixed 30% heat extraction mode demonstrated low economic performance, as the heat supply is directed not by the price of electricity, but by a technological constraint (i.e., the heat extraction mode). As illustrated in Figure S-3, the volume of electricity and heat transactions remains constant, regardless of the cost level. The variances in NPV across the cases (within the Fixed 30% heat dispatch scenario) primarily stem from a marginal increase in the heat price (see Figure S-2B and D). Improved economics, compared to the BAU scenario, were only observed in cases where heat prices exceeded a threshold that encompassed both the equivalent heat value and the additional capital costs (in $/MWht). These thresholds were identified as $19/MWht (not included in Figure S-2A) and $16/MWht in ERCOT and PJM, respectively.

In all heat price ranges, a variable 0-30% heat dispatch mode generally led to a positive change in NPV in both the ERCOT and PJM markets, demonstrating its robust marketability even at lower heat price levels ($7/MWht for ERCOT and $10/MWht for PJM, respectively; see Figure S-2A and C). The lower threshold in ERCOT is due to its greater electricity price volatility compared to PJM. Interestingly, with higher heat prices, the heat transactions monotonically increase, approaching the transaction levels observed in cases with a fixed 30% heat extraction mode (see Figure S-3). In this particular scenario, the operational flexibility was largely governed by the existing turbine rather than TES. Consequently, TES sizing would likely increase to complement the flexibility needs in maximizing electricity and heat sales revenue if constraints are imposed on the heat extraction rate (MWth). Our sensitivity analysis also indicated that a high heat price level (> $13/MWht) may render the TES system unnecessary because all available heat could be dispatched without intermediate storage.

Not surprisingly, imposing a minimum heat dispatch constraint for the last scenario resulted in poorer economics. Separate cases were considered in which the minimum required heat supply was 500 MWt and 800 MWt. These constraints can be translated into 14% and 22% heat dispatch, respectively. At high price levels, notably at $13/MWh, positive or near positive delta NPVs were obtained. However, there was a noticeable decrease in mean NPVs by 1.5 - 10.8% in ERCOT and 0.4- 7.4% in PJM, compared to its counterpart within the Variable 0-30% extraction scenario. This trend of decreasing NPVs is more pronounced at lower heat price ranges.

Figure S-4A plots the mean NPV of the different scenarios as a function of heat price for the ERCOT interconnection and shows that the variable heat dispatch scenarios provided the highest NPVs. The numbers adjacent to the data points in Figure S-4 indicate the minimum heat dispatch constraint. As heat price increases to $16/MWht, the NPVs of the scenarios that imposed a minimum heat dispatch constraint approached those of the variable heat dispatch scenarios. Figure S-4B shows similar trends for the PJM interconnection, although with lower mean NPVs.

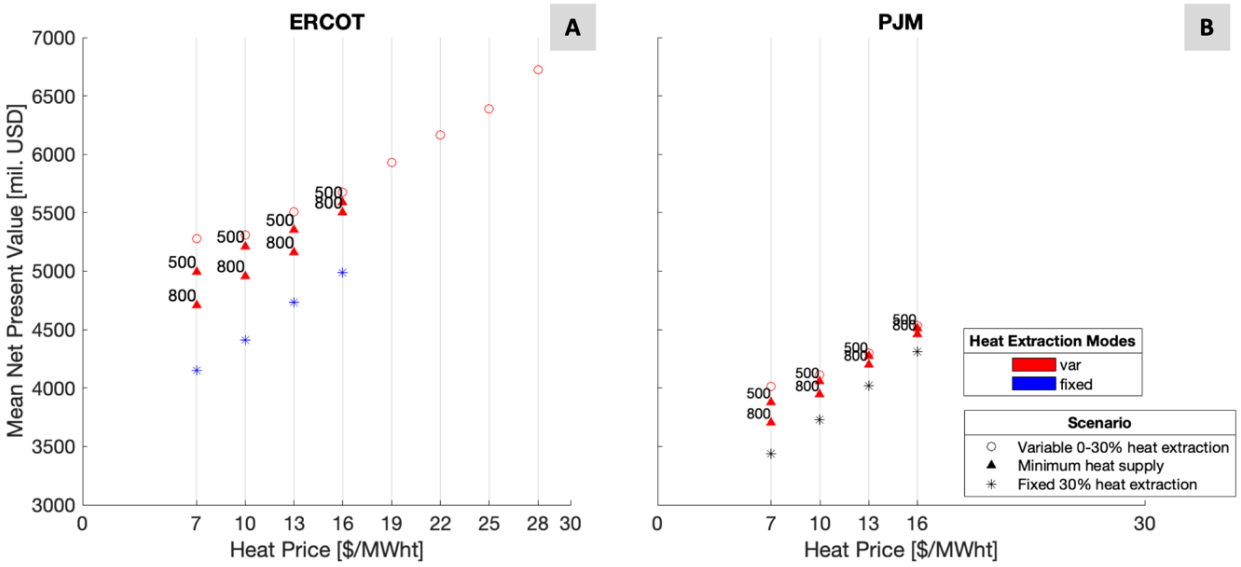

Figure S-4. Trade-offs between NPV and minimum heat supply.

CONTENTS

FIGURES

TABLES

Page intentionally left blank

ACRONYMS

BAU	business as usual
BEA	Battelle Energy Alliance, LLC
BOP	balance of plant
DOE	Department of Energy
DP	differential pressure
ERCOT	Electric Reliability Council of Texas
FWH	feedwater heater
HERON	Holistic Energy Resource Optimization Network
HDR	heat diversion ratio
HPT	high-pressure turbines
HTF	heat-transfer medium
HX	heat exchanger
IHEX	intermediate heat exchanger
INL	Idaho National Laboratory
LPT	low-pressure turbines
MS	main steam
MSDT	moisture separator drain tank
MSR	moisture separator reheater
NPV	net present value
PJM	PJM Interconnection, LLC (formerly Pennsylvania–New Jersey–Maryland Interconnection)
PWR	pressurized water reactor
RAVEN	Risk Analysis Virtual Environment
RTE	round-trip efficiency
SMR	small modular reactor
TES	thermal energy storage
TRL	technology readiness level
VRE	variable renewable energy

Page intentionally left blank

Evaluating Energy Storage Options and Costs for Consistent Energy Supply to Non-Electric Sectors

1. INTRODUCTION

This report summarizes the different options for coupling thermal energy storage (TES) systems to a pressurized light water reactor (PWR) and assesses the competitiveness of PWR-TES systems by examining selected coupling technologies under varying plant operation modes and market conditions. Therefore, the objective of this study to derive key plant performance requirements and determine heat price thresholds at which nuclear heat becomes competitive.

TES technologies can improve the dispatchability and marketability of PWR plants enabling flexible plant operations. Previous works led by the Department of Energy's (DOE's) Light Water Reactor Sustainability (LWRS) Program identified key impacts of 30% thermal power extraction on a generic Westinghouse 4-loop PWR design. The assessments include subcomponent level transients due to startup and shutdown of thermal extraction (e.g., turbines, condensers, and pumps) as well as corresponding performance [1]. Additionally, Idaho National Laboratory (INL) evaluated the competitiveness of sensible TES at various temperatures from existing and advanced nuclear reactor designs for different non-electric applications [2, 3]. With its proven technical maturity, sensible TES can be readily tailored for specific use cases by selecting an appropriate heat-transfer medium (HTF) [4].

Depending on short-term and long-term goals in coupling PWR and sensible TES systems, integrated PWR-TES systems can provide several benefits: (1) serving as a fail-safe measure by providing thermal inertia, (2) ensuring high dispatchability by carrying over stored thermal energy for later use, and (3) improving the capacity factor from net electricity sales (when compared to load-following operation mode or constant operation at reduced power output) [5, 6]. To support ongoing DOE's effort studying flexible nuclear systems and related TES technologies this report assesses sensible TES options for PWR plants focusing on two molten salt two-tank technologies.

2. MODEL DESCRIPTION

2.1 30% Extraction Considerations

The reference plant modeled for this study is based on 4-loop Westinghouse PWR design which represents 75% of all operating PWRs in the U.S [7]. This report considers a reactor with a thermal power rating of 3,650 MWt with a thermal extraction case of 30% (approximately 1,095 MWt). Extracting 30% of the reactor heat from downstream of the high pressure turbine would result in unacceptable plant disturbances [1,2]. Main steam extraction is illustrated in Figure 1. The extracted steam is routed to the TES systems via an intermediate heat exchanger (IHEX). This IHEX couples the TES system and the reactor, directing the steam into the hot tank. Following the IHEX, the extracted steam is condensed and subcooled before returning to the main power cycle. Previous studies performed a thermal analysis on the reference model and evaluated the high-level design impacts of a 30% thermal extraction. Key performance metrics of the steam extraction system are listed in Table. 1, and impacts on the nuclear plant due to thermal power extraction are listed in Table 2. Additional details regarding the assessment are presented in [1].

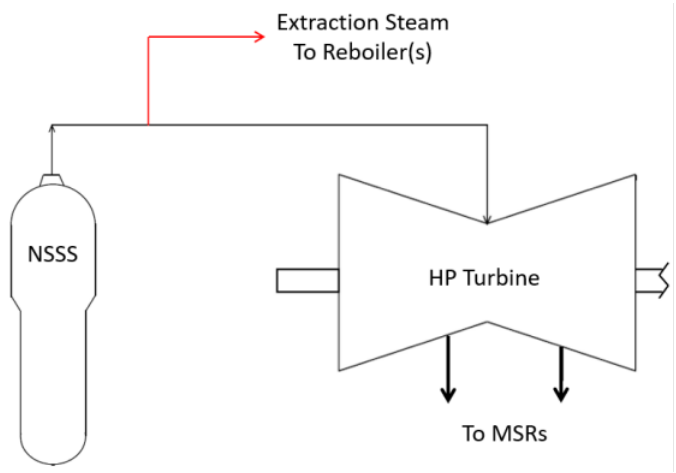

Figure 1. Steam extraction from upstream of the HP turbine [1].

Table 1. Pressure and temperature losses associated with new steam components for 30% thermal power extraction [1].

Description	Units	30% Extraction
Temperature of the condensed and subcooled extraction steam	°F/°C	120/48.9
Discharge pressure for the water supply pump	psia/kPa	650/4481.6
Pressure drop in the IHEX	psid/kPa	50/344.7
Main steam extraction differential pressure (DP)	Pounds/in.^{2} differential (psid)/kPa	80/551.6
Main steam extraction heat loss	British thermal units/hour (BTU/hr)/kW	210,000/61.5
Process steam extraction DP	Psid/kPa	100/689.5
Process steam extraction heat loss	BTU/hr/kW	2,230,000/653.3

Table 2. High-level design impacts for 30% reactor thermal power extraction [1].

Description	Units	0% Extraction	30% Extraction	Difference
Generator electric power	MWe	1,228.0	844.6	-31.2%
Thermal power extracted	MWt	0	1,095	—
% of main steam (MS) flow	%	0	21.9	—
MS flow from steam generator	Mass Per Hour (lbm/hr), kg/s	16,037,390, 2020.7	15,436,290, 1944.9	-4%
HPT inlet flow	lbm/hr, kg/s	15,218,400, 1917.5	11,272,260, 1420.3	-26%
HPT 1st stage pressure	psia, kPa	651.5, 4492.0	487.5, 3361.2	-25%
Moisture separate reheater (MSR) inlet pressure	psia, kPa	190.3, 1312.1	140.2, 966.6	-26%
Low pressure turbine (LPT) inlet flow	lbm/hr, kg/s	3,673,069, 462.8	2,677,248, 337.3	-27%
LPT inlet pressure	psia, kPa	175.5, 1210.0	129.3, 891.5	-26%
Condenser duty	BTU/hr, kW	8.21E+09, 2.40E+06	5.78E+09, 1.69E+06	-30%
Condensate pump flow	lbm/hr, kg/s	11,334,490, 1428.1	11,723,820, 1477.2	3%
Heater drain pump flow	lbm/hr, kg/s	4,732,792, 596.3	3,742,365, 471.5	-21%
Feed water heater (FWH) pump flow	lbm/hr, kg/s	16,067,280, 2024.4	15,466,190, 1948.7	-4%
Final FWH temperature	°F, °C	440.9, 227.2	413.3, 211.8	-27.6
Cascading drain flow to condenser	lbm/hr, kg/s	817,619, 103.0	745,815, 94.0	-9%
Cogen heat exchanger (HX) inlet mass flow	lbm/hr, kg/s	—	3,376,114, 425.4	—
Cogen HX inlet pressure	psia, kPa	—	817.3, 5635.1	—
Cogen HX inlet temperature	°F, °C	—	520.7, 271.5	—
Cogen HX outlet pressure	psia, kPa	—	120.0, 827.4	—

2.2 PWR-TES Coupling Considerations

While TES systems cover a wide array of heat inputs by utilizing different storage materials and energy conversion techniques, this study focuses solely on the heat-to-heat type conversion (from the energy source to the stored energy). This approach has the advantage of scalability and applicability. However, future studies may consider heat-to-electricity conversion (e.g., batteries) or electricity-to-heat conversion (e.g., firebrick storage) depending on the specific use cases. Several TES approaches are suggested for near-term nuclear integration, which include sensible storage in both solid media (i.e.,

concrete energy storage) and liquid media (i.e., two-tank liquid sensible heat storage and thermocline liquid sensible heat storage) [8, 9]. Among these technologies, the main benefit of two-tank configurations is that the hot and cold HTF is stored separately. This separation ensures constant power and temperature throughout the entire charge and discharge process, which simplifies the control and operation of the system [6, 10]. In this study, two-tank sensible TES designs are considered, due to their benefits including low-cost potential, high technology readiness level (TRL), and the ability to integrate with existing or advanced nuclear reactor systems [3]. From a market potential and safety perspective, we further refine our scope of work by considering the use of molten salts as HTF in two-tank TES systems because of the unique thermo-physical characteristics of molten salts, such as high volumetric heat capacity and low viscosity. Moreover, as demonstrated in solar thermal demo plants, they can be heated to medium- and high-temperature ranges (200-600 °C) in low-pressure operating conditions, eliminating the need for massive pressure vessels, pipe restraints, and containment buildings [11, 12].

2.2.1 Preselection of molten salts for PWR-TES coupling

The use of molten salts as a HTF is largely dependent on the operational conditions of the nuclear heat source. PWR plants generally operate at lower temperatures, which lead to a lower extracted steam temperature of 271.5°C that is then routed to the IHEX, as can be seen in Table 2 under the Cogen HX inlet temperature. Subsequently, it is crucial to keep the temperature of the cold storage tank approximately 40-100 °C above the melting point of the salts to prevent any issues related to salt freezing [3]. Other parameters crucial in choosing salts as HTFs include thermal stability, heat capacity, viscosity, thermal conductivity, and cost [13-15]. These values are acquired experimentally for specific use cases or through suppliers during the procurement processes. Therefore, tailored experimental data and a detailed bottom-up cost estimation approach are essential during the investment-grade down-selection process [16-18]. The relevant salt properties considered in this study are summarized in Table 3.

These unique considerations narrow the potential options for molten salts for PWR-TES coupling. The salts that meet these constraints are summarized in Table 4. Based on simulation and experimental studies that suggest various corrosion mitigation strategies, all the salts listed in Table 4 have been identified as suitable for use in solar thermal plants operating below 400°C [19-22].

Table 3. Key salt properties in down-selecting candidate HTFs.

Property	Related to	Unit	Note
Melting point	Minimum operation temperature, freeze protection, thermal expansion (tank, piping), heat insulation	[ºC]	The relatively high melting point of solar salt (220ºC) requires additional tank and piping insulation or the implementation of freezing protection or heat monitoring systems.
Thermal stability	Maximum operating temperature	[ºC]	Nitrate-based salts, which include chemical compounds with formulas KNO_3, $NaNO_3$, and NaNO, decompose into gaseous products at higher temperatures. This decomposition leads to an increase in pressure and a decrease in the performance of the TES system.
Specific heat	Storage capacity (amounts of heat stored)	[kJ/kg.K]	In sensible TES system, the amount of heat stored is directly proportional to its specific heat capacity and temperature difference between the hot and cold tank.
Density	Volumetric storage capacity, loading on the storage tanks and piping	[kg/m^3]	The difference in densities amongst the preselected salts for PWR applications is relatively small.
Viscosity	Pumping of the HTF	[mPa ·s]	When modifying existing thermal loops in PWR plants (as opposed to replacing them), viscosity can be an important design consideration for a molten salt TES system.
Thermal conductivity	Heat transfer, heat exchanger, steam generator	[W/m ·K]	While thermal conductivity can influence the selection of heat exchangers and steam generators, the three most commercially used salts for solar plants (Hitec, Hitec XL, and Solar salts) display a similar value of approximately 0.5.
Cost	Investment decision	[$/kg] [$/MJ]	When assessing the economic performance of salts, measures such as $/MJ or $/kWh can be utilized.

NOTE: *Surface tension can be an important consideration as it influences the pumping loads and the loading on the piping. Several studies literature suggest that surface tension can be factored in during seismic events, as it affects wave motion and sloshing inside the tanks and pipes [14]. However, this aspect was not included in this report.*

Table 4. Key properties of preselected molten salts.

Salt	Composition/ wt %	Melting point [ºC]	Stability limit (Max. operation temp.) [ºC]	Specific heat (Sensible heat storage) [kJ/kg.K]	Density [kg/m³]	Viscosity [mPa ·s]	Thermal conductivity [W/m ·K]	Cost [$/kg] /[$/MJ]	Ref.
Hitec	$NaNO_3$-KNO_3-$NaNO_2$/ 7-53-40	142	535 450-538	1.38 @180°C 1.56 @300° C	2007 @100°C 1640-1860 @300°C	3.16 @300°C	0.49-0.50@142 ºC	0.93,1.93/ 4.02	[3, 23, 24]
Hitec XL	$NaNO_3$- KNO_3-$Ca(NO_3)_2$/ 7-45-48	120	500 480-505	1.45@300° C	1992 @300°C	6.37 @300°C	0.52@120-520 ºC	1.19,1.66/ 3.58	[3, 11, 23, 25, 26]
Solar Salt	$NaNO_3$-KNO_3/ 60-40	222 220	600	1.47 @180°C 1.50 @300°C 1.56	1790	1.31-1.60 3.26 @300°C	0.51-0.60 0.5 @250-300 ºC	1.3/2.65	[3, 11]
$LiNaKNO_3$	$LiNO_3$-$NaNO_3$-KNO_3 / 30-18-52	118	550 600	1.65 @350°C 1.63	1822 @350°C	2.51 @350°C 1.50	-	1.1/1.61	[15, 27-29]
$LiNaKCaNO_3$	$LiNO_3$-$NaNO_3$-KNO_3-$Ca(NO_3)_2$ /15.5-8.2-54.3-22	93	450	-	1518	-	-	0.7/1.29	[27, 30, 31]
Lithium nitrate	$LiNO_3$	253	-	1.44	1781	7.469	0.51	-	[14, 32]

NOTE: *Reported values obtained under conditions far exceeding the operating temperature of PWR-TES systems (> 400°C) were not included in the table.*

2.2.2 PWR-two tank molten salt TES system configurations – case studies

With the rise of variable renewable energy (VRE), flexible and technically viable coupled nuclear-TES plant designs have been proposed. Carlson et al. suggested an arrangement where the TES system is integrated within the primary cycle of the Westinghouse AP1000 nuclear power plant, rated at 1050 MWe [33]. In this layout, the TES system is placed between the steam generator and the turbine, receiving its charge from the diverted steam exiting the steam generator. The stored energy is released to form steam, which is then expanded in the low pressure turbine (LPT) based on the electricity demand. Parallel designs have been explored by Frick et al., where the TES system is interconnected to a small modular reactor (SMR) [34].

Another variation includes the integration of Solar voltaic with the PWR-type SMR (160MWt), with an additional electric heater assisting TES charge [35]. For a PWR-type SMR with similar design parameters, Rigby et al. suggested using a solar parabolic trough to aid feed water heating of the SMR, which, in turn, enhances the Rankine cycle efficiency [36]. Additionally, redirecting the TES discharge to a dedicated power cycle for TES was considered in several studies [37-39]. A key advantage here is that the turbines in the primary power cycle would not require modifications and operate off-design during base load operations.

Saeed et al. and Alameri et al. considered a directly coupled TES system that separates the turbine cycle from the reactor island [3, 40]. This setup enables a direct and independent discharge of heat to both the balance of plant and the primary ranking power cycle. Recently, studies conducted by INL have comprehensively evaluated each of the nuclear-TES coupling options across various markets. Detailed findings from these investigations can be found in the reports [3, 41].

Building on the research foundation laid by a previous study [1], we selected two coupling options that minimize the impacts on existing PWR plants. As depicted in Figure 2A, the first coupling option includes a discharging configuration that separates the primary reactor loop from the stored nuclear heat applications, herein represented as a dedicated balance of plant (BOP)**.** For non-electric applications, the secondary BOP is replaced with an IHEX that is directly connected to a single heat consumer or a group of homogeneous heat users (as demonstrated in Figure 2B). In each of the coupling configurations, the TES molten-salt system was designed to maintain the HTF in the cold tank at 180°C. The first approach involves redirecting heat from the primary BOP during the charging cycle to heat the fluid flowing from the cold tank to the hot tank. A secondary steam Rankine power generation system, dedicated to TES, is used during the discharge cycle [3]. Alternatively, upgrading the existing turbine and configuring it as a single oversized BOP could be considered, rather than introducing a secondary BOP. Research suggested that, with minor modifications, the existing turbine system can accommodate a mass flow rate of 108% to 115% of its designed capacity [42, 43]. However, this approach would change the heat balance results displayed in Table 2, suggesting it as a potential area for additional research [37].

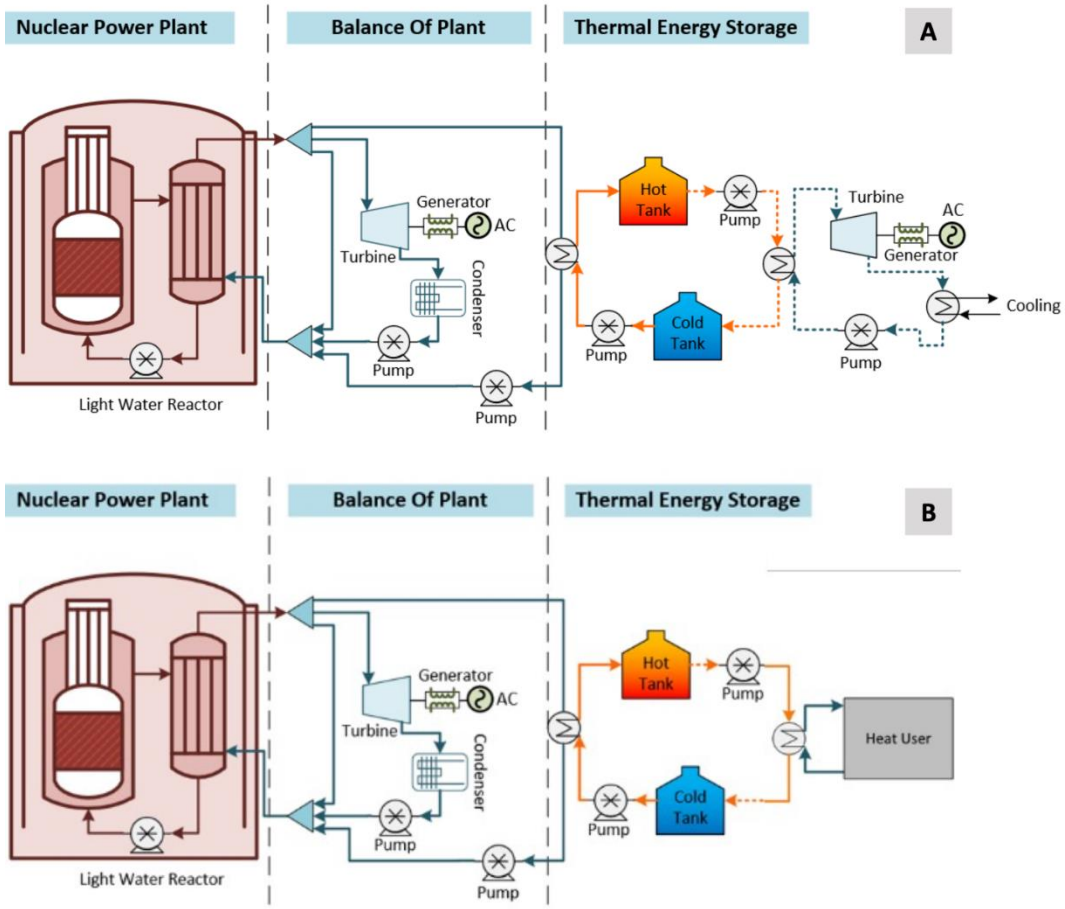

Figure 2. Proposed coupling options for the TES-integrated nuclear plant utilizing single-phase heat-transfer charging with a dedicated BOP (top) and a dedicated IHEX for a heat user (bottom) [3].

2.2.3 Bilateral heat energy market for homogenous industrial users

In this study, we assumed a single heat consumer or a group of homogeneous heat users that require a similar quality of heat in terms of both temperature and pressure. Table 5 explores possible market positioning for PWR-TES systems in heat and electricity dual markets. We considered both fixed and variable heat extraction operations. Contrary to electricity markets, characterized by multiple buyers and sellers, heat energy transactions typically occur via bilateral contracts at a fixed price between the supplier and user. As such, we position PWR-LWR systems in competitive electricity markets, seeking energy arbitrage opportunities through bilateral heat contracts. This study prioritizes heat markets characterized by minimum heat demand and unrestricted selling capacity. In these heat market settings, homogeneous heat consumers were assumed to own their own boilers and have the ability to control their outputs, implying that PWR-TES system can sell all units of extracted heat energy at the fixed heat price. However, given specific demand profiles or industrial heat consumers of interest, both static (constant heat demand) and dynamic (scheduled heat demand) scenarios can be explored.

Table 5. The heat extraction modes and their implications of introducing TES in scenarios of heat procurement at a fixed price within an electricity market with variable pricing.

Heat extraction modes	Constant heat demand	Scheduled heat demand	Minimum heat demand [b]	Unrestricted heat selling capacity [2]
Fixed 30% extraction	No energy arbitrage opportunities for TES[1]	Market potential for TES	Market potential for TES	Market potential for TES
Variable 0-30% extraction	Market potential for TES[3]	Market potential for TES	Market potential for TES	Market potential for TES

[1] *Any fixed demand lower than 1095 MWt (i.e., 30% thermal power) is not feasible for a fixed 30% extraction scenario unless a TES system with a secondary BOP or an oversized turbine is implemented (to balance excess heat energy), which is not the focus of this current analysis. However, TES might still be necessary to provide a buffer or physical barrier between the nuclear plant and industrial users.*

[2] *We assume that the heat consumers have their own self-sufficient boilers and are interested in purchasing nuclear heat to lower their costs or fulfill their carbon reduction goals. This implies that PWR-TES systems can sell all units of extracted heat energy at a predetermined fixed price without any restrictions.*

[3] *Even with a constant heat demand and a fixed heat price, there can still be opportunities for energy arbitrage. These opportunities become viable if the constant heat demand does not exceed the maximum heat that can be extracted from the primary cycle and if the heat is priced lower than the electricity price at a given time, including the thermal-to-electric conversion efficiency of 33.6%. For example, direct sales of heat to industrial consumers could be more profitable at a price of \$10/MWht as long as the electricity price remains over \$29.7/MWhe (calculated as* $\$10/MWt \times \frac{100}{33.6}\frac{MWht}{MWhe}$*).*

3. EVALUATION FRAMEWORK

The Risk Analysis Virtual ENvironment (RAVEN) and Holistic Energy Resource Optimization Network (HERON) frameworks were used to conduct an extensive stochastic analysis of PWR-TES coupled systems within the ERCOT and PJM markets. In this analysis, the primary economic drivers are electricity price signals and discrete levels of heat prices. The PWR primary loop and its existing BOP remain fixed while components integral to the coupling—namely, the charging, discharging (including secondary BOP considerations), and TES supersets—are evaluated for a range of capacity values, as shown in Table 6). Capital expenditures are calculated based on the range of superset cost functions using the polynomial cost function values in Table 7. Therefore, our investigation is specifically directed towards the incremental variations in net present value (NPV) due to possible additional investments in installing charge, discharge, and TES supersets. More information on RAVEN and HERON modeling, as well as input electricity price signals for ERCOT and PJM, is available in [3, 41].

The analysis includes 40 cases that are based on five possible scenarios: (1) a PWR plant operating as Business as Usual (BAU) with no TES; (2) a PWR-TES with a separate turbine-generator system for electricity-only markets (no thermal power dispatch); directly supplying industrial heat customers with stored heat energy from (3) fixed and (4) variable thermal power dispatch operations, and (5) heat dispatch is constrained to always remain above a minimum threshold of either 500 or 800 MWt to meet customer needs. Table 8 presents the key parameters for these scenarios, which are denoted as BAU, TES + BOP, Fixed 30% heat extraction, Variable 0-30% heat extraction, and Min. heat dispatch constraint, respectively. In all scenarios, a project lifetime of 30 years was assumed for the capital recovery period across all superset investments, along with a discount rate of 8%. It is important to note in this analysis that market intercomparison does not reflect policy considerations, market expectations, or transmission constraints. Instead, these factors are regarded *a posteriori* as represented by the electricity price signals used in HERON runs.

Table 6. Optimization variable resolution for the HERON analyses.

Variable	Range, [increment]
PWR	3650 MWt (fixed)
Primary BOP	3650 MWt (fixed)
Charge	1095 MWt (fixed)
Discharge*	1095–13140 MWt, [1095 MWt]
TES	1095–13140 MWht, [1095 MWht]

***NOTE:** This applies only to the scenario with TES that includes a secondary BOP. As mentioned in Section 2.2.3, in situations where heat is directly sold to industrial customers, the discharging power capacity [MWt] is not a variable to be optimized. This implies that all stored heat energy from TES can be delivered to industrial customers within a simulation time step (1-hour) if energy arbitrage opportunities exist.

Table 7. Cost function constants for the three superset models for the PWR-TES coupling [3].

Superset model	A	D'	X	Mean absolute percentage error
Charge	2,964,480.3	72.57 MWt	0.95986969	0.2%
TES	36,452,122.8	435.42 MWht	0.83976343	4.2%
Discharge*	10,896,427.1	72.57 MWt	0.69183838	0.8%

***NOTE:** In the cost function for the discharge superset that we used, turbine costs for electricity generation are included. Thus, when stored heat is sold directly to industrial customers without a secondary BOP, no capital expenditure for the delivering heat to customers via the discharge superset was assigned. This setting implicitly assumes that PWR-TES systems are integrated into an existing heat delivery network. Depending on the ownership of the PWR-TES systems and the structure of the heat market, detailed cost functions for the discharge superset (without a BOP consideration) need to be evaluated.

Table 8. Modeled scenarios for different markets, technological assumptions, and simulation settings.

Scenario	Market	Heat price [$/MWht]	Minimum heat supply to industrial customers [MWt]	Storage charge duration [hour]
BAU	ERCOT	-	-	-
	PJM	-	-	-
TES + BOP[1]	ERCOT	-	-	-
	PJM	-	-	-
Fixed 30% heat dispatch	ERCOT	7, 10, 13, 16	0	1-12 hours with 1-hour intervals
	PJM	7, 10, 13, 16	0	1-12 hours with 1-hour intervals
Variable 0-30% heat dispatch	ERCOT	7, 10, 13, 16, 19, 22, 25, 28	0	1-12 hours with 1-hour intervals
	PJM	7, 10, 13, 16	0	1-12 hours with 1-hour intervals
Min. heat dispatch constraint[1]	ERCOT	7, 10, 13, 16	500, 800	1-12 hours with 1-hour intervals
	PJM	7, 10, 13, 16	500, 800	1-12 hours with 1-hour intervals

[1] *The heat extraction models for TES+BOP and Min. heat dispatch constraint scenarios were allowed to vary within their constraints.* **NOTE:** Segment length of 120 hours (dispatch time horizons) was employed for HERON. Our previous research demonstrated that these 120-hour segment lengths can reasonably capture the dynamics of TES while balancing modeling accuracy and computational resource [41]; TES was modeled with a round-trip efficiency (RTE) of 90%, and incorporates a periodic condition, thus ensuring a fixed storage level (i.e., 75% TES capacity) at both the start and end of each segment length.

4. RESULTS AND ANALYSIS

4.1 General Comparison

Table 9 and Figure 3 summarize trends and key parameters across the ERCOT and PJM markets for the modeled scenarios. By examining all the combinations of capacities listed in Table 6, the cases showing the highest net present value (NPV) are presented for each scenario. Each row (representing individual market partitions) is contrasted with the corresponding Base scenario and TES+BOP scenario to highlight the potential economic advantages derived from adopting a TES for industrial heat supply. Our analysis centered on reconfiguring the existing reactor plant design into TES+PWR systems. Thus, the figure presents the extra capital investments required for this transition, clarifying the absence of corresponding optimal capacities (located at the top of Figure 3A and Figure 3D) and costs in the minus NPV column for the Base scenario and the TES+BOP scenario (Figure 3B and Figure 3E).

The design with TES and secondary BOP for peak electricity dispatch showed more economic potential in the ERCOT market compared to its BAU scenario, resulting in a positive change in NPV. The same configuration in the PJM market resulted in a negative change in NPV due to the relatively low electricity prices in the PJM market. In both markets, the capital recovery of the TES+BOP system is limited by the low thermal-to-electric conversion efficiency of the secondary BOP (27.53%). For designs in which the optimal TES capacity is equivalent to a 1-hour charge duration or 1095 MWht, the TES system operates primarily as a buffer. The heat dispatched to the TES is quickly delivered to industrial customers, rather than being stored for future energy arbitrage purposes. Optimized scenarios for which the TES capacities were greater than 1095 MWht were typically obtained at price points where the costs of heat and electricity were approximately equivalent. This result suggests that upgrading to an oversized turbine, which can utilize high-temperature steam thus increasing its efficiency while saving on capital investments in BOP, might be a preferable to the dedicated secondary BOP configuration, especially in markets characterized by lower electricity prices.

Across all markets, a fixed 30% heat extraction mode demonstrated low economic performance. As illustrated in Figure 3C and Figure 3F, the volume of electricity and heat transactions remains consistent, regardless of the cost level. The variances in NPV across the cases (within the Fixed 30% heat extraction scenario) primarily stem from a marginal increase in the heat price. Generally, TES was sized at 1095 MWht, mainly acting as a buffer (not as an energy arbitrage player). However, at a $16/MWht level, the optimal size increased to 3285 MWht in ERCOT. This trend was not evident in PJM due to its lower electricity price volatility. Delta NPV turned positive at heat price levels of $19/MWht (not included in Table 9 and Figure 3) and $16/MWht in ERCOT and PJM, respectively. This is because the opportunity cost of allocating heat to electricity generation outweighed the cost of selling heat to industrial consumers below these heat price levels, which were mainly determined by the mean electricity prices. Table 10 presents the mean electricity prices for each market along with their equivalent heat value, based on the thermal-to-electric conversion efficiency of the existing BOP (33.64%). Therefore, in cases with a fixed 30% heat extraction mode, positive delta NPV can only be guaranteed when heat prices exceed a threshold that combines both the equivalent heat value and the additional capital costs ($/MWht). This suggests that in order for a fixed heat supply from TES-PWR systems to be economically viable, a high relative value of heat is necessary. For instance, when the electricity price is low or even negative, there is less incentive to convert heat into electricity. As such, the value of the heat increases in its original form. Similarly, when heat is highly priced, the relative value of heat compared to electricity directly increases. This could be influenced by various market factors, such as high demand, limited supply, or industrial consumers who are willing to pay a premium for heat.

With the ability to regulate heat allocations between the electricity market and industrial consumers, PWR-TES systems attained economic competitiveness at heat prices of $7/MWht for ERCOT and $10/MWht for PJM, respectively, as listed in Table 9. The lower threshold in ERCOT is due to its greater electricity price volatility compared to PJM. Interestingly, PWR-TES systems outperformed the TES +

BOP scenario, resulting in a higher mean NPV at a heat price of $10/MWht within the PJM market. Specifically, with higher heat prices, the heat transactions monotonically increase, approaching the transaction levels observed in cases with a fixed 30% heat extraction mode (see Figure 3C and Figure 3F). In this particular scenario, the operational flexibility is largely governed by the existing turbine rather than the TES system. Consequently, TES sizing would likely increase to complement the flexibility needs in maximizing electricity and heat sales revenue if constraints are imposed on the heat extraction rate (MWth) or heat diversion ratio (HDR).

Table 9. HERON-optimized cases for the PWR-TES coupling.

Market	Scenario	Heat price [$/MWht]	Capacity of TES discharge (MWht, MWt)		Mean NPV [mil. USD]	Delta NPV[1] [mil. USD]/[% difference]	
ERCOT	BAU	-	-	-	5172	-	-
	TES+BOP	-	13140	12045	6326	1154	22.3
	Fixed 30% heat dispatch	7	1095	-	4153	-1019	-19.7
		10	1095	-	4413	-760	-14.7
		13	1095	-	4736	-436	-8.4
		16	3285	-	4989	-184	-3.6
	Variable 0-30% heat dispatch	7	1095	-	5278	106	2.0
		10	2190	-	5309	137	2.6
		13	1095	-	5510	337	6.5
		16	1095	-	5679	506	9.8
PJM	BAU	-	0	0	4111	-	-
	TES+BOP	-	4380	4380	4103	-7	-0.2
	Fixed 30% heat dispatch	7	1095	-	3440	-671	-16.3
		10	1095	-	3729	-381	-9.3
		13	1095	-	4020	-91	-2.2
		16	1095	-	4311	201	4.9
	Variable 0-30% heat dispatch	7	1095	-	4011	-100	-2.4
		10	1095	-	4113	2	0.1
		13	1095	-	4301	190	4.6
		16	1095	-	4533	423	10.3

[1] *Delta NPV:* $\Delta NPV = NPV_{case} - NPV_{BAU}$

***NOTE:** The capacities across all cases for the PWR, primary BOP, and charge superset were established at 3650 MWt, 3650 MWt, and 1095 MWt, respectively.

Table 10. Comparison of mean electricity price and equivalent heat value for ERCOT and PJM.

Market	Mean electricity price [$/MWhe]	Equivalent heat value [$/MWht] [1]
ERCOT	41.28	13.89
PJM	34.01	11.44

[1]*The equivalent heat value is determined by multiplying the mean electricity price by the efficiency, factoring in the thermal-to-electric conversion efficiency of the existing turbine (33.64%). This represents the opportunity cost of supplying 1 MWht of heat instead of generating electricity for electricity market sales.*

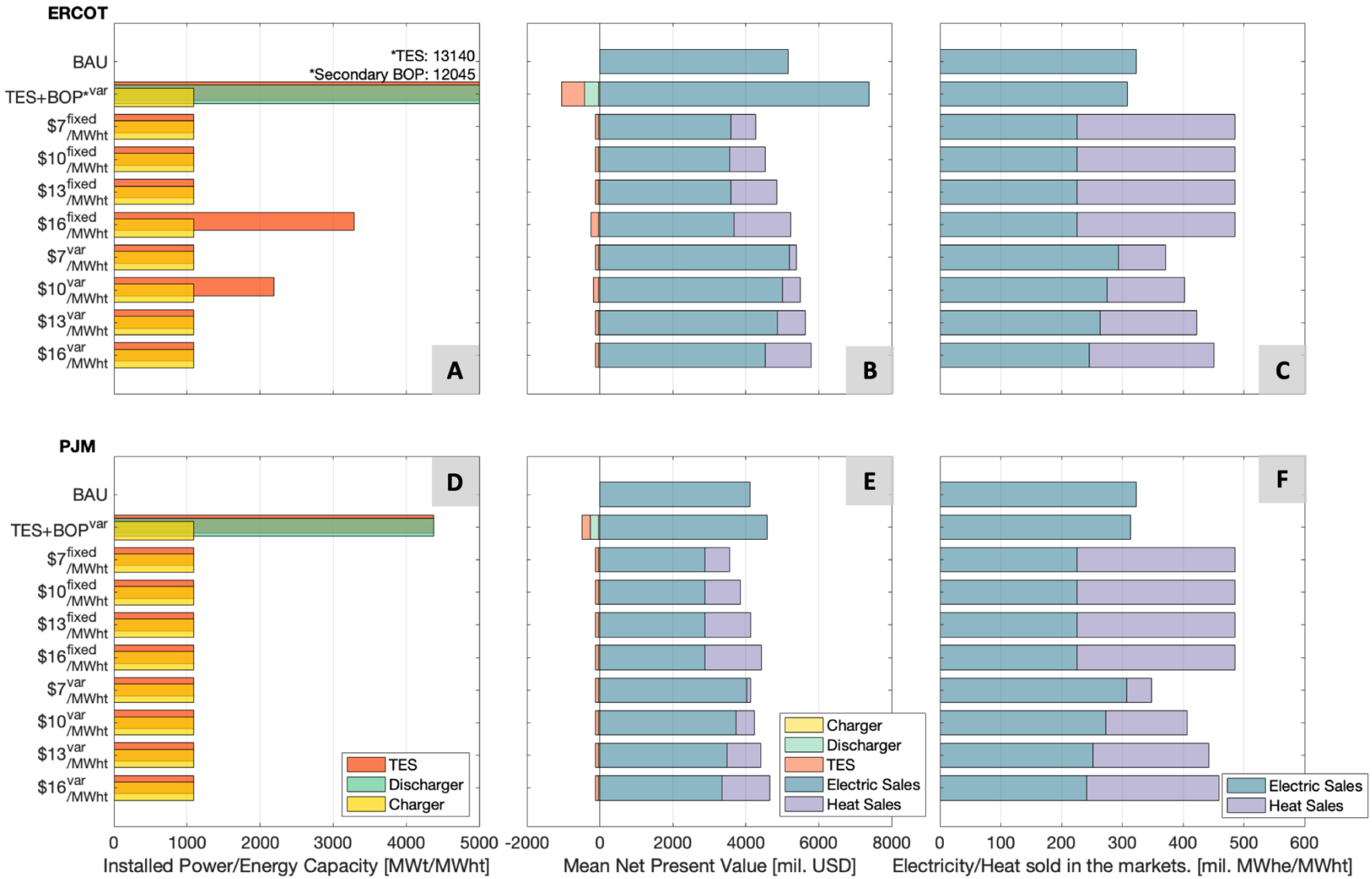

Figure 3. HERON-optimized cases for the PWR-TES coupling superset capacity (left), NPV (middle), and energy transaction (right). Note that the scenarios for "Fixed 30% heat extraction" and "Variable 0-30% heat extraction" are denoted as 'fixed' and 'var' in superscript, respectively; The heat extraction mode for TES+BOP is set at a variable range of 0-30% (denoted as ‘var’ in superscript).

4.2 Impact of Heat Prices

The optimization strategies for PWR-TES systems can be categorized into two approaches based on the ownership structure: (1) a scenario where the PWR-TES plant is owned by the industrial customer who has the goal is to minimize the cost to meet energy demands (both heat and electricity), and (2) a scenario where the PWR-TES plant and the industrial customer are distinct entities with the intention of maximizing profit for each specific entity [44]. In this research, we considered the latter ownership structure, projecting that existing PWR owners are likely to explore market potentials for industrial consumers beyond merely electricity markets.

As highlighted in Section 4.1, the optimization of a PWR-TES plant largely depends on three factors: (1) the projected heat price levels, (2) the TES capacity, and (3) the optimal heat extraction mode (when the plant is operated in a variable 0-30% heat extraction mode). Additionally, the variable heat extraction mode demonstrates its economic versatility in adapting to different heat price levels across the two markets. We focus on the impacts of heat prices on NPV and heat transactions by examining extended heat price levels for the Variable 0-30% heat extraction scenario, including a range of heat prices from \$7/MWht to \$28/MWht (see Table 11 and Figure 4).

Counterintuitively, increased heat price levels do not necessarily result in larger optimal TES capacities. In fact, as the heat price level predominantly exceeds mean electricity prices (> \$13.89/MWht; see Table 10), all TES capacities were sized at 1095 MWht. This is because there are frequent instances where selling heat directly to industrial consumers could yield more profit compared to the generation of electricity, thereby reducing the benefit of TES. While one might anticipate a heat price level of \$28/MWht to outperform the TES+BOP scenario in terms of NPV values, it remains unlikely that industrial consumers would purchase heat energy at a cost exceeding the average electricity price of the considered market. Given these considerations, TES may be required at a price level where the costs of heat and electricity are roughly equivalent, and the electricity price is volatile enough to add extra TES capacities. This supposition is backed by the cases with a \$16/MWht heat price level within the Fixed 30% extraction scenario and a \$10/MWht heat price under the Variable 0-30% heat extraction scenario (as denoted as '$\$16^{\text{fixed}}_{/\text{MWht}}$' and '$\$10^{\text{var}}_{/\text{MWht}}$' respectively in Figure 4). It is noteworthy that, at the heat price level of \$16/MWht, there were comparable amounts of electricity transactions to the grid, irrespective of the turbine heat extraction mode. However, the employment of a variable heat extraction mode resulted in a 23.7% increase in electric sales revenue compared to its counterpart in the Fixed 30% heat extraction scenario. This increase, as discussed in Section 4.1, is primarily attributed to the existing BOP actively adjusting the heat extraction ratio in response to electricity price signals, thereby maximizing opportunities for energy arbitrage (see '$\$16^{\text{fixed}}_{/\text{MWht}}$' and '$\$16^{\text{var}}_{/\text{MWht}}$' cases in Figure 4).

Table 11. Impacts of heat price level on optimal sizing and NPV in ERCOT.

Market	Scenario	Heat price [$/MWht]	Capacity of TES, discharge (MWht, MWt)		Mean NPV [mil. USD]	Delta NPV[1] [mil. USD]/[% difference]	
ERCOT	BAU	-	-	-	5172	-	-
	TES + BOP	-	13140	12045	6326	1154	22.3
	Variable 0-30% heat extraction	7	1095	-	5278	106	2.0
		10	2190	-	5309	137	2.6
		13	1095	-	5510	337	6.5
		16	1095	-	5679	506	9.8
		19	1095	-	5930	757	14.6
		22	1095	-	6168	996	19.2
		25	1095	-	6392	1220	23.6
		28	1095	-	6722	1549	30.0

[1] Delta NPV: $\Delta NPV = NPV_{case} - NPV_{BAU}$

***NOTE:** The capacities across all cases for the PWR, primary BOP, and charge superset were established at 3650 MWt, 3650 MWt, and 1095 MWt, respectively.

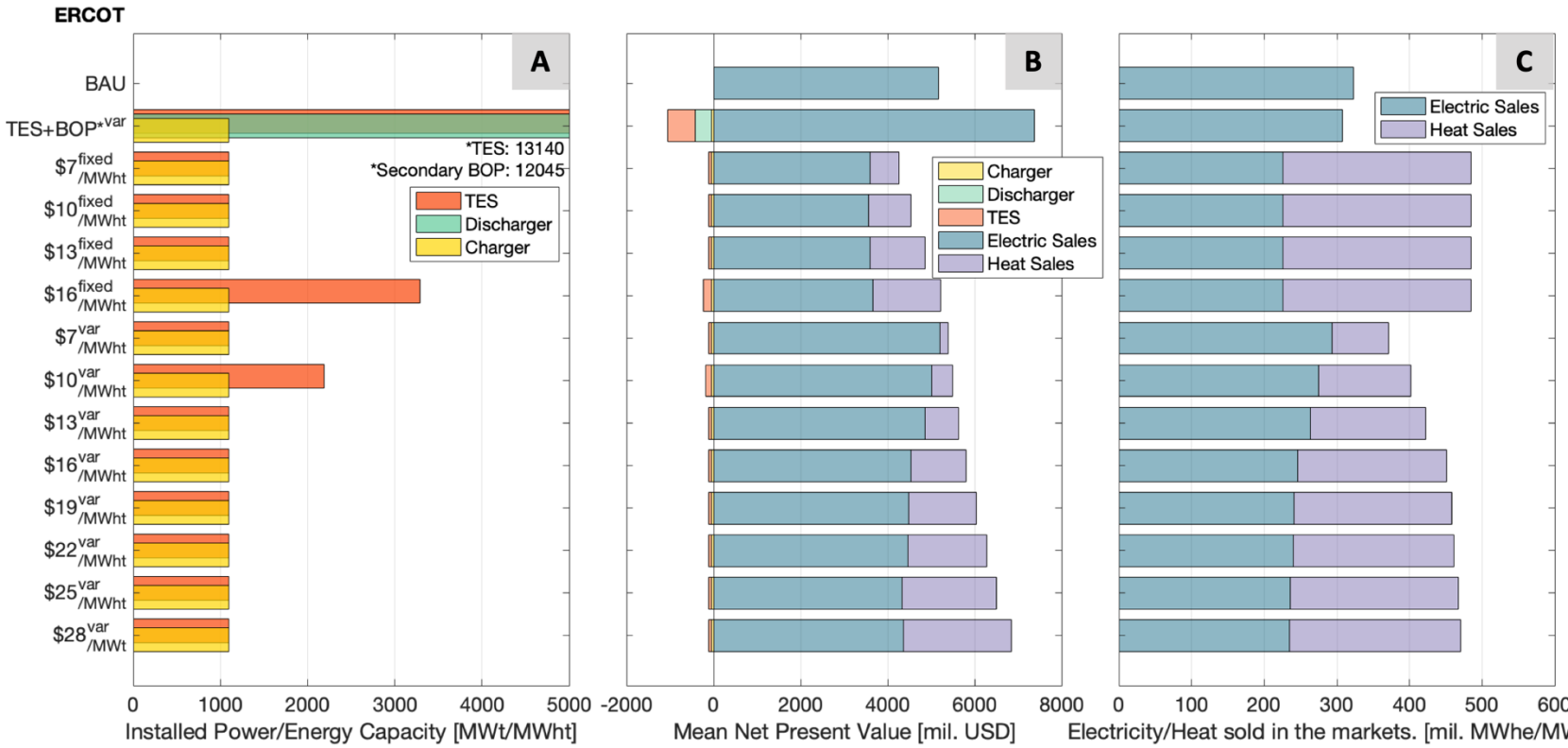

Figure 4. Impacts of a heat price level on optimal superset capacity (left), NPV (middle), and energy transaction (right). Note that the scenarios for "Fixed 30% heat extraction" and "Variable 0-30% heat extraction" are denoted as 'fixed' and 'var' in superscript, respectively; The heat extraction mode for TES+BOP is set at a variable range of 0-30% (denoted as ‘var’ in superscript

4.3 Impact of Minimum Heat Dispatch Constraints

Not surprisingly, imposing a minimum heat dispatch constraint for the last scenario resulted in poorer economics. Separate cases were considered in which the minimum required heat supply was 500 MWt and 800 MWt. These constraints can be translated into 14% and 22% heat extraction, respectively. Table 12 and Figure 5 summarize the results. Cases within the scenario of variable 0-30% heat extraction are provided as a basis for comparison. At high price levels, notably at $13/MWh, positive or near positive delta NPVs were obtained. However, there was a noticeable decrease in mean NPVs by 1.5 - 10.8% in ERCOT and 0.4- 7.4% in PJM. This trend of decreasing NPVs is more pronounced at lower heat price ranges.

Our analysis further reveals that as the heat price increases, the tradeoff relation between cases across the scenarios becomes prevalent, leading to converging heat sales and heat transactions. Hence, the differences observed in the NPVs primarily originate from variations in electricity sales (see Figure 5B and Figure 5C for ERCOT; Figure 5E and Figure 5F for PJM). Figure 6A plots the mean NPV of the different scenarios as a function of heat price for the ERCOT interconnection and shows that the variable heat dispatch scenarios provided the highest NPVs. Figure 6B shows similar trends for the PJM interconnection, although with lower mean NPVs. The numbers adjacent to the data points in Figure 6 indicate the minimum heat dispatch constraint. At a $10/MWht heat price, a case with a 500 MW minimum heat supply constraint showed less than a 2% difference in NPV in contrast to its counterpart within the Variable 0-30% extraction scenario (see Figure 6A). At $16/MWht, a case with 800MW minimum heat supply aligns with corresponding cases, showcasing an approximately 3% NPV variation. In the PJM market, due to its relatively low electricity price level (or high equivalent heat value), this convergence became noticeable at lower price levels; at $13/MWht, all cases with minimum supply constraints showed an NPV difference of less than 2.5% when compared to a case with no heat supply constraint (see Figure 6B). This indicates that in a high heat price range, there is significant market potential to couple a variety of industrial consumers with PWR-TES systems, specifically those with diverse heat supply demands.

Table 12. Impacts of a minimum heat supply level on optimal sizing and NPV in ERCOT.

Market	Scenario	Minimum heat supply [MWt]	Heat price [$/MWht]	Capacity of TES, discharge (MWht, MWt)		Mean NPV [mil. USD]	Delta NPV[1] [mil. USD]/[% difference]	
ERCOT	Variable 0-30% heat extraction	0	7	1095	-	5278	106	2.0
			10	2190	-	5309	137	2.6
			13	1095	-	5510	337	6.5
			16	1095	-	5679	506	9.8
	Minimum heat supply	500	7	2190	-	4995	-178	-3.4
			10	1095	-	5213	40	0.8
			13	1095	-	5354	181	3.5
			16	1095	-	5592	420	8.1
		800	7	2190	-	4710	-463	-8.9
			10	1095	-	4957	-215	-4.2
			13	1095	-	5162	-11	-0.2
			16	2190	-	5504	331	6.4
PJM	Variable 0-30% heat extraction	0	7	1095	-	4011	-100	-2.4
			10	1095	-	4113	2	0.1
			13	1095	-	4301	190	4.6
			16	1095	-	4533	423	10.3
	Minimum heat supply	500	7	1095	-	3879	-231	-5.6
			10	1095	-	4055	-56	-1.4
			13	1095	-	4272	161	3.9
			16	1095	-	4513	402	9.8
		800	7	1095	-	3706	-405	-9.9
			10	1095	-	3946	-165	-4.0
			13	1095	-	4201	90	2.2
			16	1095	-	4462	351	8.5

[1] Delta NPV: $\Delta NPV = NPV_{case} - NPV_{BAU}$

***NOTE:** The capacities across all cases for the PWR, primary BOP, and charge superset were established at 3650 MWt, 3650 MWt, and 1095 MWt, respectively.

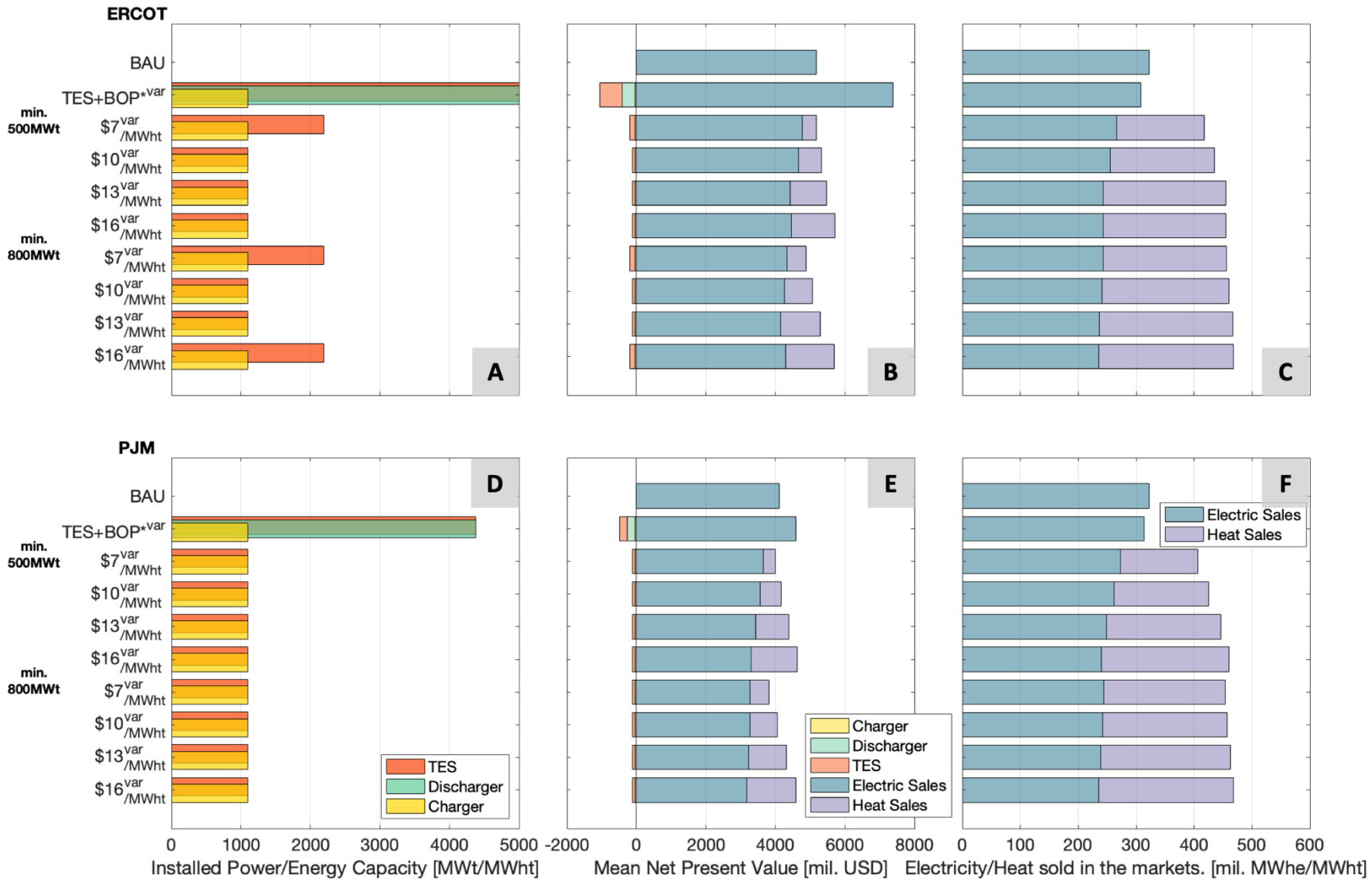

Figure 5. Impacts of a minimum heat supply level on optimal superset capacity (left), NPV (middle), and energy transaction (right). Note that the scenario for "Variable 0-30% heat extraction" are denoted as 'var' in superscript; The heat extraction modes for TES+BOP and Minimum heat supply scenarios are set at a variable range of 0-30% (denoted as ‘var’ in superscript).

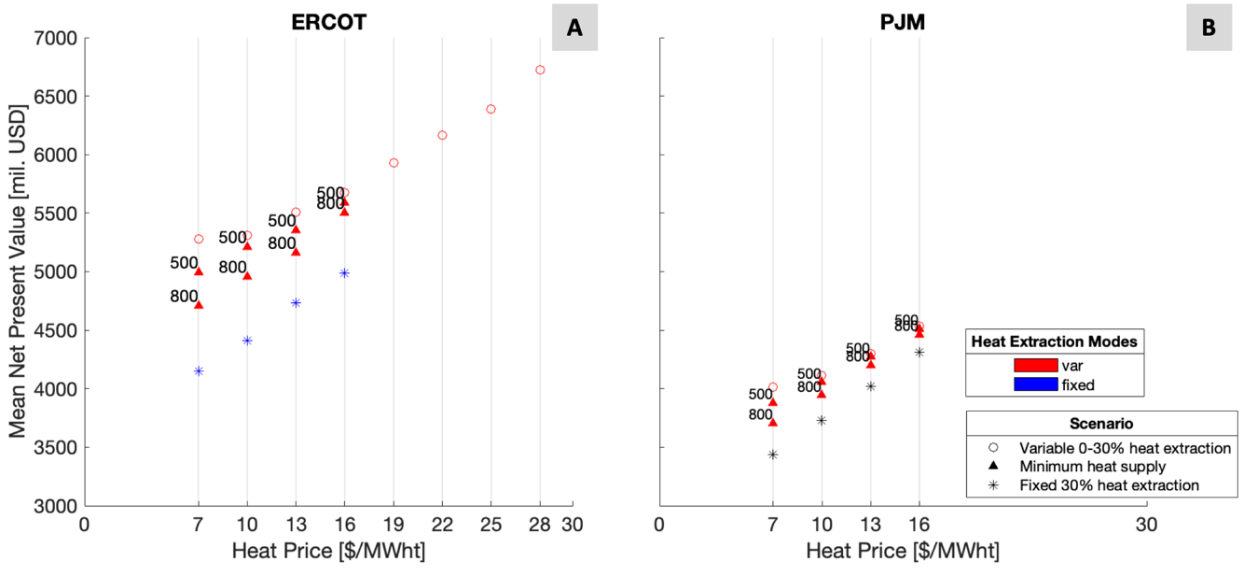

Figure 6. Trade-offs between NPV and minimum heat supply: As the heat price increases, regions showing similar NPV values between cases with different minimum heat supply levels were observed, suggesting increased flexibility in pairing industrial consumers with PWR-TES systems at high heat price. Note that in the scenario of minimum heat supply, the applied minimum heat supply levels were indicated above the respective data points. No minimum heat supply constraint was imposed for cases with a variable 0-30% heat extraction mode, in other words, the minimum supply level is zero.

5. CONCLUSIONS AND FUTURE WORK

Non-electric applications of nuclear heat have attracted interest as a cleaner alternative to conventional process heat traditionally sourced by fossil fuels. This study bears three objectives. First, our goal is to offer a comprehensive guide defining key criteria for the selection of TES technologies for this purpose. We used the heat balance analysis results obtained from extracting 30% of reactor heat from a 4-loop Westinghouse PWR plant as a reference design. Building upon previous research on TES, we identified a two-tank molten salt TES design as the most feasible option for providing nuclear heat to industrial customers. Secondly, we aimed at evaluating the competitiveness of PWR-TES systems across a wide range of technological pathways, including different modes of heat delivery (i.e., fixed vs. variable heat delivery) and varying types of industrial customers (i.e., those with and without minimum heat supply requirements). Finally, our objective was to measure sensitivity and identify optimal market conditions conducive to the proposition of PWR-TES systems. For this analysis, ERCOT and PJM were chosen as proxy markets, representing a high electricity price and volatility scenario and a low electricity price and low volatility scenario.

Using the cost functions and the dispatch optimizing tool, HERON, the cost-optimal interaction between technological constraints and optimal superset capacities, and various performance attributes was derived. This includes the optimal TES capacity, projected mean NPV, electricity and heat transactions. Our findings revealed that economics of PWR-TES systems are largely determined by mean electricity of the market where the PWR-TES systems are introduced. This effect is more pronounced when the plant operates in a fixed 30% heat extraction mode, as the heat supply is directed not by the price of electricity, but by a technological constraint (i.e., the heat extraction mode). This finding holds in cases where the minimum heat requirements are in place. When the optimal TES capacity is sized to accommodate a 1-hour charge duration, equivalent to 1095 MWht, the TES system typically operates as a buffer. The heat diverted to the TES is immediately delivered to industrial customers, rather than being stored for future energy arbitrage purposes.

In our sensitivity analysis, we observed a complementary relationship between the heat extraction mode and optimal TES capacities in terms of providing heat allocation flexibility to either BOP or industrial customers. Results showing an optimal TES capacity greater than 1095 MWht were typically obtained at price points where the costs of heat and electricity were approximately equivalent. These findings were particularly prominent in cases where a fixed heat extraction mode was utilized in the ERCOT market, characterized by high electricity prices and high volatility.

In all heat price ranges, a variable 0-30% heat extraction mode generally led to a positive change in NPV in both the ERCOT and PJM markets, demonstrating its robust marketability. However, when extraction of heat is variable, dictated by market-specific electricity price signals, the optimal heat transactions to industrial customers tend to be smaller than their counterparts under the fixed 30% mode. This implies that if industrial customers demand more than this transaction level (i.e., the economically deliverable amount of heat that leads to optimal NPV), the economics of the PWR-TES plant will decrease. This is due to the reduced opportunities associated with converting heat into electricity and selling it to the grid at higher prices instead. Our observations also indicated a high heat price level (> $13/MWht) resulted in heat transaction levels similar to those seen with a fixed 30% heat extraction mode, thus reducing the need for TES. These insights could provide valuable guidance for integrating PWR-TES systems with industrial consumers, particularly those with diverse heat requirements.

For future work, including the thermophysical and cost representation of emerging molten salts, such as $LiNaKNO_3$, $LiNaKCaNO_3$, and Lithium Nitrate, cost functions will ensure that TES is valued properly in providing heat for industrial consumers. Parallel enhancements in heat balance analysis for variable 0-30% extraction and discharge cost functions (when TES is directly coupled to industrial consumer, excluding a secondary BOP) will enable a more accurate economic assessment for PWR-TES plants. Lastly, market potential for PWR-TES systems can be expanded with considerations for upgrading current turbines to maximize energy arbitrage opportunities, thus ensuring the viability of these systems even in low-electricity price markets.

6. REFERENCES

[1] T. Westover, H. R. Fidlow, H. Gaudin, J. Miller, G. Neimark, and N. Richards, "Impacts of Extracting 30% of Reactor Power from a Pressurized Water Reactor," Idaho National Lab.(INL), Idaho Falls, ID (United States), 2023. [Online]. Available: https://lwrs.inl.gov/Flexible%20Plant%20Operation%20and%20Generation/Screening-30percent-TPD-Impacts.pdf

[2] M. Green *et al.*, "Nuclear hybrid energy system: molten salt energy storage," *Idaho Falls, Idaho, USA: Idaho National Laboratory,* 2013.

[3] R. M. Saeed *et al.*, "Multilevel Analysis, Design, and Modeling of Coupling Advanced Nuclear Reactors and Thermal Energy Storage in an Integrated Energy System," Idaho National Lab.(INL), Idaho Falls, ID (United States), 2022.

[4] H. Balliet, L. McLaughlin, Z. Ma, and K. Glusenkamp, "Technology Strategy Assessment: Findings from Storage Innovations 2030 Thermal Energy Storage," Idaho National Laboratory (INL), Idaho Falls, ID (United States), 2023.

[5] S.-B. Cho, A. S. Epiney, P. W. Talbot, X. Sun, and T. Allen, "Study of Storage Requirements and Costs for Shaping Renewables and Nuclear Energy: FY23 Summary Report," Idaho National Laboratory (INL), Idaho Falls, ID (United States), 2023.

[6] R. Gabbrielli and C. Zamparelli, "Optimal design of a molten salt thermal storage tank for parabolic trough solar power plants," 2009.

[7] T. L. Westover *et al.*, "Preconceptual Designs of Coupled Power Delivery between a 4-Loop PWR and 100-500 MWe HTSE Plants," Idaho National Laboratory (INL), Idaho Falls, ID (United States), 2023.

[8] R. M. Saeed, K. L. Frick, A. Shigrekar, D. Mikkelson, and S. Bragg-Sitton, "Mapping thermal energy storage technologies with advanced nuclear reactors," *Energy Conversion and Management,* vol. 267, p. 115872, 2022.

[9] J. Coleman, S. Bragg-Sitton, and E. Dufek, "An evaluation of energy storage options for nuclear power," Idaho National Lab.(INL), Idaho Falls, ID (United States), 2017.

[10] T. Bauer, C. Odenthal, and A. Bonk, "Molten salt storage for power generation," *Chemie Ingenieur Technik,* vol. 93, no. 4, pp. 534-546, 2021.

[11] E. González-Roubaud, D. Pérez-Osorio, and C. Prieto, "Review of commercial thermal energy storage in concentrated solar power plants: Steam vs. molten salts," *Renewable and sustainable energy reviews,* vol. 80, pp. 133-148, 2017.

[12] J. Edwards, H. Bindra, and P. Sabharwall, "Exergy analysis of thermal energy storage options with nuclear power plants," *Annals of Nuclear Energy,* vol. 96, pp. 104-111, 2016.

[13] H. Kim, J. Seo, Y. A. Hassan, J. Yoo, S. Qin, and J. L. Hartvigsen, "Evaluation and selection of eutectic salts combined with metal foams for applications in high-temperature latent heat thermal energy storage," *Journal of Energy Storage,* vol. 76, p. 109790, 2024.

[14] S. Ladkany, W. Culbreth, and N. Loyd, "Molten salts and applications I: Molten salt history, types, thermodynamic and physical properties, and cost," *J. Energy Power Eng,* vol. 12, pp. 507-516, 2018.

[15] A. Bonk, S. Sau, N. Uranga, M. Hernaiz, and T. Bauer, "Advanced heat transfer fluids for direct molten salt line-focusing CSP plants," *Progress in Energy and Combustion Science,* vol. 67, pp. 69-87, 2018.

[16] R. M. Saeed *et al.*, "Industrial Requirements Status Report and Down-Select of Candidate Technologies," Idaho National Laboratory (INL), Idaho Falls, ID (United States), 2023.

[17] A. Abou Jaoude, C. Bolisetti, L. Lin, L. M. Larsen, A. S. Epiney, and E. K. Worsham, "Literature Review of Advanced Reactor Cost Estimates," 2023.

[18] A. Abou-Jaoude, Y. Arafat, A. W. Foss, and B. W. Dixon, "An Economics-by-Design Approach Applied to a Heat Pipe Microreactor Concept," Idaho National Lab.(INL), Idaho Falls, ID (United States), 2021.

[19] G. García-Martin, M. I. Lasanta, M. T. de Miguel, A. I. Sánchez, and F. J. Pérez-Trujillo, "Corrosion Behavior of VM12-SHC Steel in Contact with Solar Salt and Ternary Molten Salt in Accelerated Fluid Conditions," *Energies,* vol. 14, no. 18, p. 5903, 2021.
[20] F. Pedrosa, T. Marcelo, C. Nogueira, A. Gomes, and T. Cunha Diamantino, "Molten nitrate salts containing lithium as thermal energy storage media: a short review," in *ECOS 2018: 31st International Conference on Efficiency, Cost, Optimization, Simulation and Environmental Impact of Energy Systems*, 2018: Universidade do Minho, Departamento de Engenharia Mecânica.
[21] A. G. Fernandez, F. Pineda, E. Fuentealba, D. Jullian, A. Mallco, and M. Walczak, "Compatibility of alumina forming alloys with LiNO3-containing molten salts for solar thermal plants," *Journal of Energy Storage,* vol. 48, p. 103988, 2022.
[22] A. Ibrahim, H. Peng, A. Riaz, M. A. Basit, U. Rashid, and A. Basit, "Molten salts in the light of corrosion mitigation strategies and embedded with nanoparticles to enhance the thermophysical properties for CSP plants," *Solar Energy Materials and Solar Cells,* vol. 219, p. 110768, 2021.
[23] L. T. Knighton *et al.*, "Energy Arbitrage: Comparison of Options for use with LWR Nuclear Power Plants," Idaho National Lab.(INL), Idaho Falls, ID (United States), 2021.
[24] T. Wang, S. Viswanathan, D. Mantha, and R. G. Reddy, "Thermal conductivity of the ternary eutectic LiNO3–NaNO3–KNO3 salt mixture in the solid state using a simple inverse method," *Solar energy materials and solar cells,* vol. 102, pp. 201-207, 2012.
[25] M. S. Sohal, M. A. Ebner, and P. Sabhar, "Engineering database of liquid salt thermophysical," Idaho National Lab.(INL), Idaho Falls, ID (United States), 2013.
[26] L. Moens, D. M. Blake, D. L. Rudnicki, and M. J. Hale, "Advanced thermal storage fluids for solar parabolic trough systems," *J. Sol. Energy Eng.,* vol. 125, no. 1, pp. 112-116, 2003.
[27] K. Vignarooban, X. Xu, A. Arvay, K. Hsu, and A. M. Kannan, "Heat transfer fluids for concentrating solar power systems–a review," *Applied Energy,* vol. 146, pp. 383-396, 2015.
[28] P. Zhang, J. Cheng, Y. Jin, and X. An, "Evaluation of thermal physical properties of molten nitrate salts with low melting temperature," *Solar Energy Materials and Solar Cells,* vol. 176, pp. 36-41, 2018.
[29] R. I. Olivares and W. Edwards, "LiNO3–NaNO3–KNO3 salt for thermal energy storage: thermal stability evaluation in different atmospheres," *Thermochimica acta,* vol. 560, pp. 34-42, 2013.
[30] Z. Jiang *et al.*, "Form-stable LiNO3–NaNO3–KNO3–Ca (NO3) 2/calcium silicate composite phase change material (PCM) for mid-low temperature thermal energy storage," *Energy Conversion and Management,* vol. 106, pp. 165-172, 2015.
[31] J. G. Cordaro, N. C. Rubin, and R. W. Bradshaw, "Multicomponent molten salt mixtures based on nitrate/nitrite anions," 2011.
[32] M. Lachheb, F. Albouchi, F. Mzali, S. B. Nasrallah, and T. Benameur, "Thermal conductivity enhancement of lino3/graphite composite for energy storage," *Int. Journal of Heat & Technology,* vol. 31, no. 2, pp. 9-16, 2013.
[33] F. Carlson, J. H. Davidson, N. Tran, and A. Stein, "Model of the impact of use of thermal energy storage on operation of a nuclear power plant Rankine cycle," *Energy Conversion and Management,* vol. 181, pp. 36-47, 2019.
[34] K. Frick, C. T. Misenheimer, J. M. Doster, S. D. Terry, and S. Bragg-Sitton, "Thermal energy storage configurations for small modular reactor load shedding," *Nuclear Technology,* vol. 202, no. 1, pp. 53-70, 2018.
[35] A. Borisova and D. Popov, "An option for the integration of solar photovoltaics into small nuclear power plant with thermal energy storage," *Sustainable Energy Technologies and Assessments,* vol. 18, pp. 119-126, 2016.
[36] A. C. G. Rigby, M. Wagner, and B. Lindley, "Dynamic Modelling of Flexible Dispatch in a Novel Nuclear-Solar Integrated Energy System with Thermal Energy Storage," *Available at SSRN 4528600,* 2023.

[37] A. Kluba and R. Field, "Optimization and exergy analysis of nuclear heat storage and recovery," *Energies*, vol. 12, no. 21, p. 4205, 2019.
[38] F. Carlson and J. H. Davidson, "Parametric study of thermodynamic and cost performance of thermal energy storage coupled with nuclear power," *Energy Conversion and Management*, vol. 236, p. 114054, 2021.
[39] E. Ingersoll, K. Gogan, J. Herter, and A. Foss, "Cost & Performance Requirements for Flexible Advanced Nuclear Plants in Future US Power Markets," LucidCatalyst LLC, Cambridge, MA (United States), 2020.
[40] S. A. Alameri, *A coupled nuclear reactor thermal energy storage system for enhanced load following operation*. Colorado School of Mines, 2015.
[41] R. M. Saeed *et al.*, "A Multidisciplinary Approach to Integrated Energy Systems: Advanced Nuclear Plants with Thermal Storage for Dynamic and Flexible Operation in Diverse Markets," Idaho National Lab.(INL), Idaho Falls, ID (United States), 2023.
[42] M. Richter, G. Oeljeklaus, and K. Görner, "Improving the load flexibility of coal-fired power plants by the integration of a thermal energy storage," *Applied energy*, vol. 236, pp. 607-621, 2019.
[43] R. Sigg, C. Heinz, M. Casey, and N. Sürken, "Numerical and experimental investigation of a low-pressure steam turbine during windage," *Proceedings of the Institution of Mechanical Engineers, Part A: Journal of Power and Energy*, vol. 223, no. 6, pp. 697-708, 2009.
[44] P. W. Talbot *et al.*, "Evaluation of Hybrid FPOG Applications in Regulated and Deregulated Markets Using HERON," Idaho National Lab.(INL), Idaho Falls, ID (United States); Electric Power …, 2020.